# Selenoxides Are Better Hydrogen-Bond Acceptors than Sulfoxides: a Crystallographic Database and Theoretical Investigation

**Eric Renault and Jean-Yves Le Questel***

*Laboratoire de Spectrochimie et Modélisation, EA 1149, FR CNRS 2465, Université de Nantes, 2, rue de la Houssinière, BP 92208, 44322 Nantes Cedex 3, France*

*Received: April 20, 2004; In Final Form: June 15, 2004*

The relative hydrogen-bond (HB) properties of sulfoxides and selenoxides have been investigated experimentally using data retrieved from the Cambridge Structural database and theoretically through density functional calculations at the B3LYP/6-311++G(3df,3pd)//B3LYP/6-311++G(3df,3pd) level. The HB are significantly shorter (stronger) in selenoxides (d(O···H) = 1.78 (3) Å) than in sulfoxides (d(O···H) = 1.85 (2) Å). The HB directionalities and linearities observed in the solid state for the two functionalities are very similar. The spatial and molecular surface minima of the electrostatic potential are, respectively, 43.9 and 23.4 kJ/mol more negative in dimethyl selenoxide (DMSeO) in comparison with that in dimethyl sulfoxide (DMSO). The investigation of the S(Se)O bond's electronic structure using the Natural Bond Orbital (NBO) approach shows that negative hyperconjugation of the type $n_O \rightarrow \sigma^*S(Se)-C$ is much more important in DMSO than that in DMSeO. In the HB complexes, the NBO analysis shows competition between $n_O \rightarrow \sigma^*S(Se)-C$ delocalizations associated to hyperconjugation and $n_O \rightarrow \sigma^*HF$ delocalizations related to hydrogen-bonding. The NBO energetic analysis of the HB complexes demonstrates that the H···O interaction is significantly greater in DMSeO compared to that in DMSO. The computed thermodynamic parameters of HB complexation support the better HB ability of selenoxides since the $\delta\Delta H^\circ_{298}$ and $\delta\Delta G^\circ_{298}$ are, for the three HB donors used (HF, $H_2O$, and *p*-fluorophenol) always significantly in favor of DMSeO. The theoretical $\delta\Delta H^\circ_{298}$ and $\delta\Delta G^\circ_{298}$ calculated for DMS(Se)O HB interactions with *p*-fluorophenol, respectively, of 8.5 and 6.0 kJ/mol, compares reasonably well with the corresponding experimental data in solution of 2.8 and 5.0 kJ/mol. The theoretical $\delta\Delta\nu$(XH) clearly confirm the various observations, the $\delta\Delta\nu$(OH) value of 111 $cm^{-1}$ calculated from the HB complexes with $H_2O$ being close to the experimental $\delta\Delta\nu$(OH) of about 110(±20) $cm^{-1}$.

## 1. Introduction

The chemistry of sulfoxides, their ability to interact with electron donating or accepting ligands, together with the controversial debate around the nature of the SO bond have led to several experimental and theoretical investigations.[1] The enthalpies of hydrogen-bonding interactions between sulfoxides and several hydrogen bond (HB) donors have, for example, been determined.[2] It is well-known from these studies that sulfoxides can be considered as strong HB acceptors. From a structural point of view, computational studies have been used to analyze the structure and HB energetics of DMSO with various donors (for example 1DMSO−$n$$H_2O$ clusters;[3] DMSO−*N*-methyl maleimide;[4] DMSO−1,2-ethanediol[5]). These studies have shown that, beside the strong HB involving the sulfoxide oxygen, the methyl groups are also involved in numerous HB.

In the solid state, Calligaris et al. have used the Cambridge Structural Database (CSD) to characterize the metrics of uncoordinated and metal-coordinated sulfoxides.[6,7] In contrast to sulfur-containing compounds, the structural and energetic HB properties of analogous organoselenium molecules have not been characterized. In a recent work, we have shown for the first time from thermodynamic measurements in solution, that selenoxides are better HB acceptors that sulfoxides.[8] In the solid state, preliminary observations of Steiner in his comprehensive compilation of the whole palette of HB[9] seems to indicate the same behavior. From a theoretical point of view, an ab initio and a density functional theory (DFT) investigation of chemical bonding in $Y_2XZ$ compounds have shed light on the bond nature in $Y_2SO$ and $Y_2SeO$ structures through the Atoms In Molecules (AIM) Theory.[10] However, to our knowledge, no specific study has been devoted to the characterization of the HB properties in SO and SeO systems and to their comparison.

In an effort to fill this gap, we complete in this paper our thermodynamic investigation in solution[8] by a comprehensive structural and theoretical study. By means of two complementary approaches, namely DFT calculations and investigation of the CSD, we will address the following questions: (1) Do the geometries of SO···H and SeO···H HB interactions in the solid state allow for the determination of the best HB acceptor? (2) Are there preferential directionalities of hydrogen-bonding interactions in these systems and are these HBs linear? (3) Can we gain insight, through quantum mechanic descriptors, into the factors responsible for the observed preference? (4) Despite the environment differences, are the trends noticed through solid state (CSD), solution (thermodynamic measurements), and gas-phase (computational methods) observations coherent?

To answer these questions, CSD searches have been carried out for diversified and comparable XYSO···HZ and XYSeO···HZ environments. The theoretical approach has first been focused on electrostatic and bond orbital descriptors of DMSO and DMSeO "free" molecules, chosen as model

* Corresponding author: E-mail: Jean-Yves.LeQuestel@chimie.univ-nantes.fr. Tel: 33 (0)2 51 12 55 63. Fax: 33 (0)2 51 12 55 67.

10.1021/jp0482870 CCC: $27.50 
Published on Web 08/03/2004

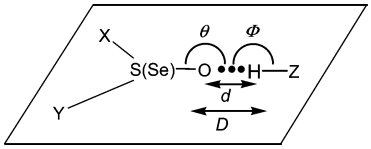


**Figure 1.** Definition of the geometric parameters describing the hydrogen-bonding interactions in XYS(Se)O molecular fragments searched in the CSD.

compounds. The thermodynamic parameters of HB interactions between DMSO, DMSeO, and various HB donors have then been computed. Finally, theoretical infrared frequency shifts have been compared to the ones measured in solution for comparable systems.

## 2. Methods

**2.1. CSD Analyses.** Crystallographic data were retrieved from the November 2003 (298 097 entries) 5.25 release of the CSD.[11] The ConQuest and QUEST3D programs[12] were used to search for bonded substructures and intermolecular nonbonded contacts in XYSO and XYSeO systems. Subsequent data analyses were performed with VISTA.[13] Searches were restricted to entries with (a) error-free coordinate sets in CSD check procedures, (b) no crystallographic disorder, (d) no polymeric connections, and (e) crystallographic *R*-factor $\leq 0.10$. All H atoms involved in nonbonded contact searches were placed in normalized positions, i.e., they were repositioned along their X-ray-determined X−H vectors at a distance from O or N equal to the appropriate mean bond length established from neutron studies.[14]

Nonbonded contact searches and geometrical analyses of interactions involving HZ (Z = N, O) hydrogen bond donors and O acceptors in XYSO and XYSeO systems have been carried out using the recommendations of Desiraju and Steiner in their recent monograph:[15] *d* and *D* (Figure 1) are, respectively, the HB lengths involving the sulfoxides and selenoxides oxygens atoms expressed from the hydrogen (*d*) and heavy atom (*D*) position of the HB donor, $\theta$ measures the linearity of the interactions, and $\Phi$ measures their directionalities. A contact was accepted as a hydrogen bond only if it was less than the sum of the van der Waals radii of the hydrogen (1.0 Å)[16] and oxygen (1.52 Å)[17] atoms: that is to say if $d \leq 2.62$ Å. The respective ranges considered for the HB linearities and directionalities were $90 \leq \theta \leq 180°$ and $90 \leq \Phi \leq 180°$. The scatterplots and the contoured density surface showing the experimental distribution of HB donors around the oxygen atoms in sulfoxides have been created using the ISOGEN program.[18]

A Student test with a 95% statistical confidence limit has been used to verify the validity of the conclusions drawn from the data analysis. Two kind of samples have been obtained through this test (i) some for which the comparison of two data (e.g., two average values) gave probabilities below 0.1 and (ii) those for which the corresponding probabilities were ranging from 0.1 to 0.8. In fact, all the distance comparisons lead to probabilities below 0.1, whereas the corresponding values for the angle comparisons were greater than 0.1. We have, therefore, only considered the differences between the various distances to be significant.

**2.2. Computational Methods.** *2.2.1. Level of Theory.* In recent years, DFT has become prominent as an accurate and computationally inexpensive means of accounting for electron correlation. Its validity for describing hydrogen bonding for very diversified HB acceptors has been shown, for example, in the systematic study performed by Rablen et al on the interactions of a single water molecule with small organic molecules.[19] Among the functionals applicable to hydrogen bonding, our choice of B3LYP,[20] which invokes Becke's three parameter hybrid method using the correlation functional of Lee, Yang, and Parr, is based on the fact that is has been shown to produce theoretical data within 1−3 kJ/mol of the MP2 results.[21]

The computations were carried out with the Gaussian 98[22] suite of programs either on local workstations or through the CINES and IDRIS computational facilities.

*2.2.2. Basis Set.* Quantum chemical calculations using B3LYP with two basis sets were performed on 1:1 HB complexes of DMSO and DMSeO with different HB donors (vide infra). We have first used the 6-311+G(**) basis set augmented in a second step by polarization functions on all atoms and diffuse functions on hydrogen atoms: 6-311++G(3df,3pd). The basis set dependence of the free base computed properties has been assessed through its comparison with the experimental data available (geometry, dipole moment). For the HB complexes, the evolution of the interaction energy has been analyzed in order to shed light on the importance of the number of polarization functions and the presence of diffuse functions on hydrogen atoms.

*2.2.3. Theoretical Descriptors.* 2.2.3.1. Free Bases. The strong electrostatic component of hydrogen bonding has led to an extensive use of charge arrangement descriptors for qualitative and quantitative HB analyses.[23] Two descriptors, $V_{min}$ and $V_{s,min}$, the spatial and molecular surface minima of the electrostatic potential, respectively, have been proven to be particularly well suited for the modeling of hydrogen-bonding interactions.[24] We have, therefore, computed the $V_{min}$ and $V_{s,min}$ of DMSO and DMSeO using a molecular surface defined[25] by an 0.001 e/bohr$^3$ isocontour of the electronic density for $V_{s,min}$. The angular location of the electrostatic potential minima has proven to be useful for the analyses of the directional preferences observed in intermolecular interactions.[26] To compare the theoretical preferences to the ones observed in the solid state, we have computed the S(Se)O $V_{min}$($V_{s,min}$) angles and have compared them to the experimental S(Se)O···H angles. These calculations have been made with the HS95 program at the B3LYP/6-311++G**//B3LYP/6-311++G(3df,3pd) level since the program does not support f functions.[27]

For a better understanding of the relative chemical bonding in SO and SeO systems, we have performed an NBO analysis[28] on DMSO and DMSeO. The principal theoretical methods available to study chemical bonding and intermolecular interactions are the NBO approach and the AIM methodology. Our choice has turned to the NBO approach since the AIM method has been used recently for comparable systems by Dobado and co-workers.[10] Furthermore, the NBO approach has proven its interest in the case of hypervalent molecules since it has been used by Reed and Schleyer in their pioneering investigation on "Chemical Bonding in Hypervalent Molecules".[29] Last, the interest of the NBO methodology to elucidate the bonding situation in hypervalent sulfur species has been confirmed very recently by Leusser et al. in the case of sulfur−nitrogen compounds.[30] In this work, we have specifically analyzed the SO and SeO bond properties through an NBO analysis in order to compare the bond's degree of polarization in these bonds. Negative hyperconjugation of the type $n \rightarrow \sigma^*$ has been invoked as one of the main characteristic of the bonding in S(Se)O containing compounds.[29] We have, therefore, selected as NBO descriptors of the SO and SeO bonds in DMSO and DMSeO the occupancies, *q*, of the donor oxygen lone pairs NBO $n_O$ and of the paired acceptor antibonding NBO ($\sigma^*_{S(Se)-C}$). We have then calculated the energetic stabilization induced by the

$n_O \rightarrow \sigma^*_{S(Se)-C}$ charge-transfer interactions in the two compounds through second-order perturbation theory according to eq 1, for a general donor NBO (*i*) and acceptor NBO (*j*):

$$E = \Delta E_{ij} = q_i \frac{F^2(i,j)}{\epsilon_j - \epsilon_i} \quad (1)$$

where $q_i$ is the $i^{th}$ donor orbital occupancy, $\epsilon_i$ and $\epsilon_j$ are diagonal elements (orbital energies), and $F$(i,j) are off-diagonal elements associated with the NBO Fock matrix. Although this procedure is known to overestimate stabilizing interactions, they closely parallel the energies afforded by the more accurate Fock matrix deletion method.[31]

*2.2.3.1. Hydrogen-Bonded Complexes.* 2.2.3.1.1. Geometries. The geometries of both monomers and HB complexes have been fully optimized at the above levels of theory. All stationary points were confirmed as true minima via vibrational frequency calculations. We have selected three HB donors: (i) HF, the smallest HB donor, which allows for the lowest computational cost,[32] (ii) *p*-fluorophenol, the reference HB donor in the building of the p$K_{HB}$ scale,[33] and (iii) $H_2O$, the standard reference HB donor in the biochemical and organic modeling community. We have not fully explored the potential energy surfaces of each HB donor around the oxygen of DMS(Se)O but rather have tried several starting geometries of complexation.

2.2.3.1.2. NBO Descriptors. The use of NBO parameters to analyze HB interactions in various systems has proven to be useful.[34] The NBO theory describes the formation of an AH···B hydrogen bond as the charge transfer from the lone pair, $n_B$, of the acceptor B into the vacant antibonding orbital, $\sigma^*$, of the HB donor AH. In this work, we have therefore analyzed, in the case of the DMSO and DMSeO hydrogen-bonded complexes with HF, the evolution of the NBO population of the oxygen lone pairs ($n_O$) and of the antibonding $\sigma^*_{HF}$ NBO. We have then computed the stabilization energy associated with the interaction $n_O \rightarrow \sigma^*_{HF}$ in the two HB complexes.

2.2.3.1.3. Thermodynamic Quantities. The interaction energies have been computed according to the supermolecule approach, that is to say the difference between the energy of the HB complex and the sum of the monomers energies. The electronic energy, $\Delta E_{el}$, the enthalpy, $\Delta H^\circ_{298}$, and the Gibbs free energy of complexation, $\Delta G^\circ_{298}$, have been respectively computed from eqs 2−4.

$$\Delta E_{el} = E_{el}\,(\text{complex}) - [E_{el}\,(\text{DMS(Se)O}) + E_{el}\,(\text{AH})] \quad (2)$$

$$\Delta H^\circ_{298} = \Delta E_{el} + \Delta E_{ZPVE} + \Delta E_{tr} + \Delta E_{rot} + \Delta E_{vib,therm} - RT \quad (3)$$

$$\Delta G^\circ_{298} = \Delta H^\circ_{298} - T\Delta S^\circ_{298} \quad (4)$$

The enthalpy includes the zero-point vibrational energies, $\Delta E_{ZPVE}$, the thermal energies which comprise the effects of molecular translation, $\Delta E_{tr}$, rotation, $\Delta E_{rot}$, and vibration, $\Delta E_{vib,therm}$, at 298.15 K and 1 atm and the $\Delta pV$ correction (equal to $-RT$ in the usual assumption of ideal gas behavior).

2.2.3.1.4. Basis Set Superposition Error. To correct the well-known spurious stabilization of the HB complex commonly referred to as the basis set superposition error (BSSE), we have used the full conterpoise method[35,36] with fragment relaxation.[37]

## 3. Results and Discussion

**3.1. CSD Studies.** *3.1.1. Observed SO and SeO Geometries.* Structure and bonding in sulfoxide complexes have been investigated in detail by Calligaris and Carugo through CSD statistical analyses.[6] A survey of SO bond lengths in 'free' and H-bonded species in this study has allowed for showing the lengthening of the SO bond upon hydrogen bonding. Comparatively, such an investigation has not been made for SeO compounds. To be able to analyze accurately the effects of HB interactions on S(Se)O distances, we have first collected the S(Se)O bond lengths for each entry in which the oxygen was not involved in hydrogen bonding. The number of entries (726 refcodes corresponding to 860 fragments) containing the 'free' SO bond has allowed us to investigate more deeply the effect of the local environment on the SO geometry. We have been able to collect CSD entries for sulfites (O−SO−O), sulfinamides (C−SO−N), and sulfoxides (C−SO−C). Such investigation of the structural variation induced by the intramolecular environment around the SeO bond has not been possible for selenoxides, owing to the low number of entries found in the CSD. Table 1 shows the values of SO and SeO bond lengths for the various fragments investigated. The mean SO bond length in sulfoxides of 1.492 (1) Å is in perfect agreement with the one found by Calligaris and Carugo,[6] the number of data collected in the present investigation being five times greater (643 instead of 101 observations). This bond length compares well with the one determined for DMSO in the gas phase by microwave spectroscopy (1.485 (6) Å),[38] gas electron diffraction data (1.484 (2) Å),[39] and recent DFT and MP2 calculations (1.514 and 1.508 Å, respectively).[10] In sulfites, Table 1 shows that the mean SO bond length is significantly shortened (1.438 (2) Å). A significant shortening is also observed for sulfinamides ($d$(SO) = 1.475 (2) Å).

**TABLE 1: Geometries Observed in the CSD for SO and SeO 'Free'[a] Molecular Fragments**

| fragment | $N_{ent}$ ($N_{obs}$)[b] | $d$(SO) (Å)[c] | $d$(SeO) (Å) |
|---|---|---|---|
| X−SO−Yc | 726 (860) | 1.483 (1) | |
| C−SO−C | 537 (643) | 1.492 (1) | |
| C− SO−N | 36 (44) | 1.475 (2) | |
| O− SO−O | 52 (58) | 1.438 (2) | |
| X−SeO−Yd | 16 (20) | | 1.64 (2) |

[a] Here, free means uninvolved in HB interactions. [b] $N_{ent}$, number of refcodes; $N_{obs}$, number of fragments observed. [c] The values in parentheses are the mean estimated standard deviations. [d] X = C, N, O; Y = C, N, O.

**TABLE 2: HB Geometrical Descriptors (Figure 1) Observed in the CSD for X−SO−Y Molecular Fragments**

| fragment | $N_{ent}$ ($N_{obs}$)[a] | $d$/(Å) | $D$/(Å) | $\theta$/(°) | $\Phi$/(°) | $d$(SO)/(Å) |
|---|---|---|---|---|---|---|
| X−SO−Y | 305 (402) | 1.85 (2) | 2.790 (8) | 128 (1) | 162 (2) | 1.502 (1) |
| C−SO−C | 270 (354) | 1.84 (1) | 2.779 (8) | 128 (1) | 162 (1) | 1.505 (1) |
| C−SO−N | 27 (38) | 2.00 (4) | 2.91 (3) | 132 (3) | 158 (4) | 1.488 (3) |

[a] $N_{ent}$, number of refcodes; $N_{obs}$, number of fragments observed.

The mean SeO bond length of 1.64 (2) Å in Table 1 is in good agreement with the 1.70 Å value reported recently by Dokarev et al. through their X-ray crystallographic investigation on DMSeO metal-coordinated complexes[40] and the ones obtained from theoretical calculations for DMSeO (DFT and MP2, 1.672 and 1.663 Å, respectively).[10]

*3.1.2. Relative Hydrogen Bonding on SO and SeO Molecular Fragments.* Among the 402 SO fragments (305 entries) engaged in HB interactions, we have found 38 HBs (27 entries) corresponding to sulfinamides and 354 HBs (270 structures) to sulfoxides. Unfortunately, no sulfite has been found involved in hydrogen bonding. Table 2 shows the mean values of the various geometrical descriptors (Figure 1) of the HBs involving SO molecular fragments. These data are consistent with the

**TABLE 3: HB Geometrical Descriptors (Figure 1) Observed in the CSD for X−SO−Y and X−SeO−Y Molecular Fragments**

| fragment | $N_{ent}$ ($N_{obs}$)[a] | $d$ (Å) | $D$ (Å) | $\theta$ (°) | $\Phi$ (°) | $d$(S(Se)O) (Å) |
|---|---|---|---|---|---|---|
| X−SO−Y | 305 (402) | 1.85 (2) | 2.793 (8) | 128 (1) | 162 (2) | 1.502 (1) |
| X−SeO−Y | 8 (10) | 1.78 (3) | 2.74 (2) | 130 (5) | 164 (3) | 1.665 (6) |

[a] $N_{ent}$, number of refcodes; $N_{obs}$, number of fragments observed.

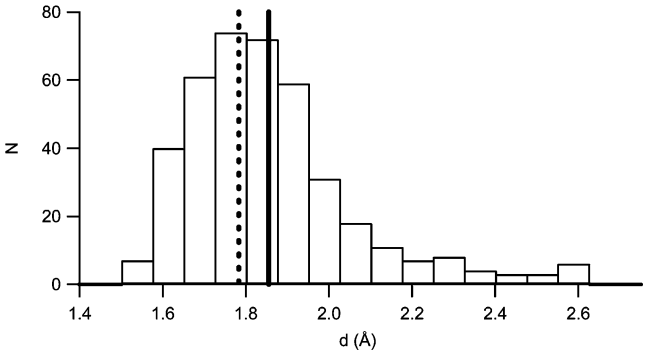


**Figure 2.** Histogram of the HB distances $d$(H···O)(Å) observed in the CSD on the oxygen of sulfoxides. The position of the mean values observed for hydrogen bonding on the oxygen of sulfoxides and selenoxides are indicated by dashed and continuous vertical lines, respectively.

behavior expected from the SO bond length variation in the 'free' fragments. Based on the HB distances, sulfinamides are weaker HB acceptors than sulfoxides. Despite the environmental differences, these crystallographic observations are in good agreement with the trends revealed from thermodynamic measurements in solution.[8]

Table 3 presents the mean geometries of the HB in SO and SeO fragments and Figure 2 shows the histogram of the HB distances in sulfoxides. The mean value of the HB distances is significantly shorter in selenoxides (1.78 (3) Å) than in sulfoxides (1.85 (2) Å), a behavior which confirms, in the solid state, the better HB ability of the SeO functionality compared to SO pointed out recently through thermodynamic measurements in solution.[8] This trend is also highlighted through the comparison of the HB distances measured for SO and SeO moieties in close chemical environments. The $d$ (D) values of 1.782 (2.749) measured for a SeO···H HB in the JEKTAU[41] crystal structure are indeed in favor of an increased HB strength compared to the corresponding values of 1.815 (2.781) measured in CONPAW[42] for a SO···H HB(Figure 3).

The $\theta$ angles observed on the oxygen atoms of sulfoxides and selenoxides can be used to investigate HB directionality at SO and SeO acceptors. The HB directionalities observed for SO and SeO moieties are very similar since the $\theta$ mean values are 128 (1) and 130 (5), respectively. It is worth noticing that they compare well with the directional preferences observed for metal(M)−oxygen coordination in sulfoxides,[6] the MOS angles having a mean value close to 120°. Figure 4 shows the experimental distribution of HB donors in sulfoxides. From this scatterplot, it appears that no mutual orientation of HO and SX-(Y) bonds is preferred. By representing this experimental distribution with isocontours based on the number of contacts (Figure 5), it is clearly seen that the trans-trans arrangement (relative to XS and YS bonds) is in fact the most abundant (Scheme 1). As observed by Calligaris and Carugo for M−O coordination in sulfoxides, this stereochemistry of interactions is indeed the one minimizing steric interactions between the approaching HB donor (or metal) and the sulfoxide side groups.[6]

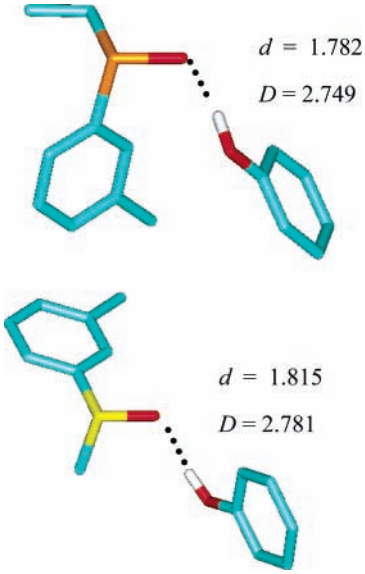


**Figure 3.** Geometric parameters observed in the CSD for HB on the oxygen of SeO (refcode, CONPAW) and SO (refcode, JEKTAU) moieties in close chemical environments.

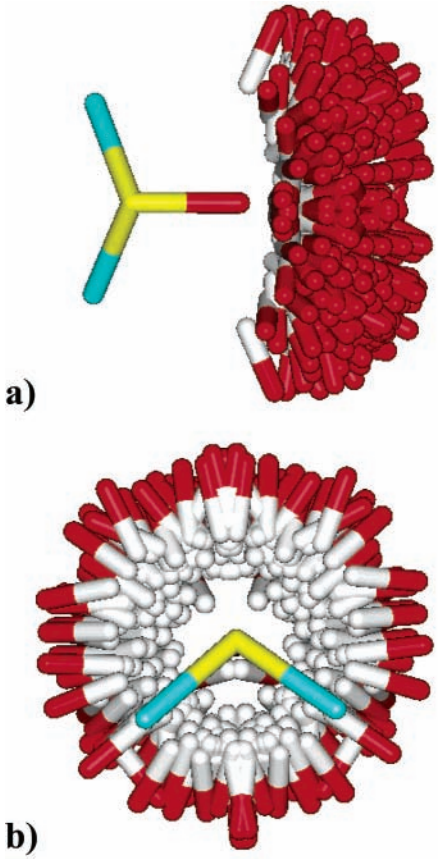


**Figure 4.** Experimental distribution of N/O−H donors around sulfoxides observed in the CSD and viewed a) in the SO bond plane and b) along the SO bond.

The very wide range of torsion angles XSe(YSe)HZ measured in the CSD for HBs on the oxygen of selenoxides, from −166 to 175°, and the low number of observations (10) does not allow us to see any preferred streochemistry in the case of SeO···HZ interactions.

The HB linearities can be assessed through the $\Phi$ angles observed for O···HO HBs on the oxygen atoms of sulfoxides and selenoxides. The mean values of 162 (2) and 164 (3)° do

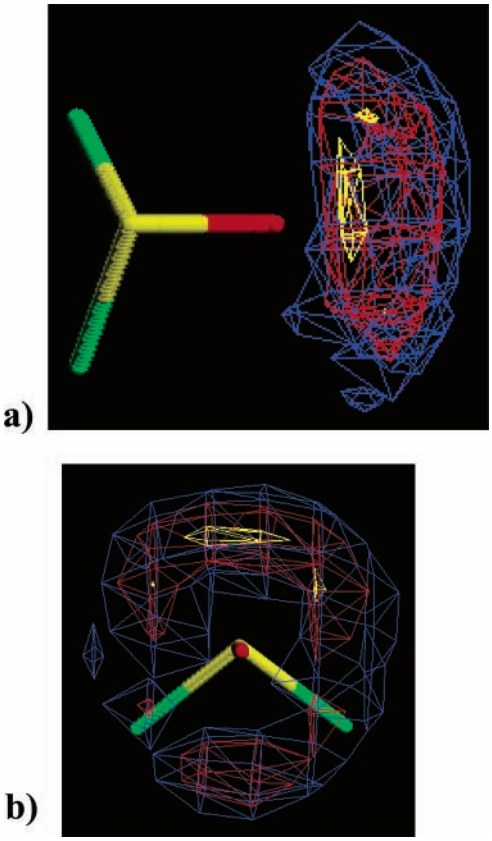


**Figure 5.** Density of HBD around sulfoxides observed in the CSD and viewed a) in the SO bond plane and b) along the SO bond.

**SCHEME 1: Trans, Cis Arrangements of the HB Donors in Sulfoxide (Relative to XS and YS Bonds)**

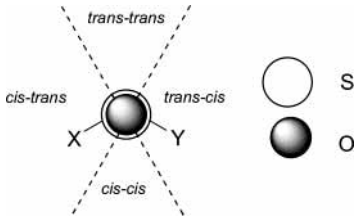


not reveal a distinct behavior of the SO and SeO moieties, such arrangements being typical of a linear geometry slightly distorted by the crystalline surrounding.

**TABLE 5: Experimental and Theoretical Dipole Moments (D) of DMSO and DMSeO**

| | | B3LYP/ 6-311+G** | | B3LYP/ 6-311++G(3df,3pd) | |
|---|---|---|---|---|---|
| compound | $\mu_{exp.}$(gas) | $\mu$ | $\Delta\mu^a$ | $\mu$ | $\Delta\mu^a$ |
| DMSO | 3.96 | 4.45 | −0.49 | 4.03 | −0.07 |
| DMSeO | | | 4.76 | | 4.52 |
| HF | 1.83 | 1.98 | −0.16 | 1.83 | −0.01 |
| $H_2O$ | 1.85 | 2.16 | −0.31 | 1.89 | −0.04 |
| *p*-fluorophenol | 2.17 | 2.14 | 0.03 | 2.02 | 0.15 |

[a] $\Delta\mu = \mu_{exp.}(gas) - \mu_{calc}$.

**3.2. Computational Studies.** *3.2.1. 'Free' DMSO and DMSeO Properties.* 3.2.1.1. Geometries. Table 4 shows the experimental and theoretical bond lengths and angles of DMSO and DMSeO. By comparing the geometrical parameters observed in the gas phase for DMSO with the ones obtained through the two basis sets used in the density functional calculations, it appears that, on going from 6-311+G** to 6-311++G(3df,3pd), the overestimation of the CS and SO bond lengths is notably reduced: from −0.028 to −0.012 Å and from −0.030 to −0.06 Å, respectively. This observation clearly supports the importance, in such hypervalent sulfur molecules, of the number of polarization and diffuse functions used in the basis set.[39] Conversely, the bond angles are perfectly reproduced with both basis sets. Since no gas phase structural data are available for DMSeO, we have used the mean of the bond lengths and angles observed in the CSD for 'free' C−SeO−C molecular fragments. The trends revealed from the comparison between the experimental data available and the theoretical results are very similar to the ones observed for DMSO, the B3LYP/6-311++G(3df,3pd) giving structural data much closer to experiment.

3.2.1.2. Dipole Moment. The experimental and theoretical dipole moment values of the two model compounds used in the present investigation are presented in Table 5. This property is a good criterion to test the applicability of a level of theory for hydrogen bonding, owing to the electrostatic nature of hydrogen bonds. The values computed at the 6-311+G** basis set are, in general, overestimated: from 0.16 (HF) to 0.49 D (DMSO). This observation again illustrates the importance of the number of polarization and diffuse functions, already noticed by various authors.[19,39] The theoretical dipole moments computed at the B3LYP/6-311++G(3df,3pd) level are generally in excellent agreement with the experimental ones, the $\Delta\mu$ range varying from 0.1 (HF) to 0.07 (DMSO) D. The only exception

**TABLE 4: Experimental and Theoretical Geometries of DMSO and DMSeO**

| | | | B3LYP/ 6-311+G** | | | B3LYP/ 6-311++G(3df,3pd) | | |
|---|---|---|---|---|---|---|---|---|
| compound | exptl[a] (gas) | exptl[b] (X-ray) | | $\Delta_1$[c] | $\Delta_2$[d] | | $\Delta_1$[c] | $\Delta_2$[d] |
| | | | | DMSO | | | | |
| | | | | Bond Lengths | | | | |
| C−S | 1.807(1) | 1.76(2) | 1.835 | −0.028 | −0.08 | 1.819 | −0.012 | −0.06 |
| S−O | 1.484(2) | 1.494(5) | 1.514 | −0.030 | −0.022 | 1.490 | −0.06 | 0.004 |
| | | | | Bond Angles | | | | |
| C−S−C | 96.6(1) | 97.9(5) | 96.5 | 0.1 | 1.4 | 96.6 | 0.0 | 1.3 |
| C−S−O | 106.6(3) | 107.0(8) | 106.8 | −0.2 | 0.2 | 106.8 | −0.2 | 0.2 |
| | | | | DMSeO | | | | |
| | | | | Bond Lengths | | | | |
| C−Se | | 1.961(5) | 1.982 | | −0.021 | 1.973 | | −0.012 |
| Se−O | | 1.656(7) | 1.672 | | −0.012 | 1.654 | | −0.002 |
| | | | | Bond Angles | | | | |
| C−S−eC | | 96.4(6) | 94.5 | | 1.9 | 94.7 | | 1.7 |
| C−S−eO | | 103.2(5) | 104.0 | | −0.8 | 103.8 | | −0.6 |

[a] Reference 39. [b] This work (cf. Table 1). [c] Difference between experimental (gas phase) and theoretical values. [d] Difference between experimental (X-ray) and theoretical values.

**TABLE 6: Energy (kJ/mol) and Angular Location of the Electrostatic Potentials Calculated[a] for DMSO and DMSeO**

| compound | $-V_{min}$ | $-V_{s,min}$ | S(Se)O···$V_{min}$ | S(Se)O···$V_{s,min}$ | S(Se)O···H[b] |
|---|---|---|---|---|---|
| DMSO | 276.0 | 203.0 | 125 | 152 | 133 (1) |
| DMSeO | 319.9 | 226.4 | 121 | 150 | 130 (5) |

[a] B3LYP/6-311++G**. [b] Mean values observed in the CSD (see Tables 2 and 3).

**TABLE 7: NBO Descriptors[a] Computed[b] for DMSO and DMSeO**

| | q | | |
|---|---|---|---|
| | DMSO | DMSeO | $\Delta q$[c] |
| $n1_O$ | 1.9934 | 1.9948 | 0.0014 |
| $n2_O$ | 1.8902 | 1.9118 | 0.0216 |
| $n3_O$ | 1.8243 | 1.8562 | 0.0311 |
| $\sigma^*_{S(Se)-C1}$ | 0.1049 | 0.1017 | −0.0032 |
| $\sigma^*_{S(Se)-C2}$ | 0.1039 | 0.1011 | −0.0028 |
| | $E_{n\rightarrow\sigma^*}$ | | |
| | DMSO | DMSeO | $\Delta E_{n\rightarrow\sigma^*}$[d] |
| $n2_O \rightarrow \sigma^*_{S(Se)-C}$[e] | 32.2 | 29.4 | −2.8 |
| $n3_O \rightarrow \sigma^*_{S(Se)-C}$[e] | 52.6 | 42.6 | −10.0 |

[a] The various descriptors are given in atomic units, and the energies are expressed in kJ/mol. [b] B3LYP/6-311++G(3df,3pd) level. [c] $\Delta q$ = $q$NBO (DMSeO) − $q$NBO (DMSO). [d] $\Delta E_{n\rightarrow\sigma^*} = E_{n\rightarrow\sigma^*}$ (DMSeO) − $E_{n\rightarrow\sigma^*}$ (DMSO). [e] The values correspond to the mean of the $n_O \rightarrow \sigma^*_{S(Se)-C1}$ and $n_O \rightarrow \sigma^*_{S(Se)-C2}$ transitions (the atom numbering refers to that used in Figure 1).

to this behavior is *p*-fluorophenol, for which the less-extended basis set leads to theoretical data in better agreement with the experimental ones.

Last, Table 5 shows that the dipole moment of DMSeO is consistently larger than that of DMSO. These data confirm the polarized character of the S(Se)O bonds and reveal a significant increase of polarization in DMSeO. They are in agreement with the greater difference in electronegativities between selenium and oxygen compared to sulfur and oxygen.[43]

3.2.1.3. Electrostatic Potentials. Table 6 gathers the $V_{min}$ and $V_{s,min}$ values of DMSO and DMSeO together with their angular locations (S(Se)O···$V_{min}$($V_{s,min}$) angles). Both parameters show the increased nucleophilic character of the oxygen in DMSeO compared to DMSO. The relative evolution of $V_{min}$ and $V_{s,min}$ between the two molecules ($\Delta V_{min}$ and $\Delta V_{s,min}$ have respective values of 43.9 and 23.4 kJ/mol) are coherent with the trends revealed through the dipole moment analysis. These data show that the increased electron density on the oxygen of DMSeO compared to DMSO contibute to the greater value of the dipole moment.

It is worth noticing through Table 6 that the angular locations of the spatial minima S(Se)O···$V_{min}$ are in good agreement with the directional preferences observed in crystalline environments.

3.2.1.4. NBO Descriptors. The energies (in atomic units) and the percentage of p character (indicated in parentheses) of the three oxygen lone pairs ($n1_O$, $n2_O$, and $n3_O$) obtained through the NBO analysis for DMSO and DMSeO are, respectively, −0.81 (24.7%); −0.28 (98.2%); and −0.27 (99.3%) and −0.84 (17.6%); −0.26 (98.3%); and −0.25 (99.4%). As our objective in this part of the discussion is the comparison of negative hyperconjugation between DMSO and DMSeO through the study of $n_O \rightarrow \sigma^*_{S(Se)-C}$ charge transfer interactions, we have only considered the NBO lone pairs having the highest energies and the highest percentage of p character. These lone pair NBOs indeed correspond to the most depleted by hyperconjugation that are significantly paired with $\sigma^*_{S(Se)-C}$ antibonding NBOs. The values of the various NBO descriptors selected are presented in Table 7. These data show that in DMSeO, the NBO related to the oxygen lone pairs are less depleted (more electron rich) than the corresponding NBO in DMSO, the population difference being 0.02158 and 0.03196 e, respectively. Concomitantly, the antibonding $\sigma^*_{S(Se)-C}$ paired orbitals are less populated in DMSeO than in DMSO, these differences being −0.0032 and −0.0028, respectively. The greater importance of hyperconjugation in DMSO compared to DMSeO is also demonstrated through the $n_O \rightarrow \sigma^*_{S(Se)-C}$ stabilization energies, always greater in DMSO than in DMSeO, the energy differences being −2.8 and −10.0 kJ/mol. The analysis of NBO descriptors of free DMSO and DMSeO reveals, therefore, valuable information of the electronic structures of the two compounds coherent with the more polarized character of the SeO bond compared to the SO one. These characteristics should be associated with a specific behavior toward HB donors.

**TABLE 8: Selected HB Parameters of the Optimized[a] Complexes of DMS(Se)O**

| | DMSO | | | DMSeO | | |
|---|---|---|---|---|---|---|
| HB donor | $d_1$/(Å) | $\theta_1$/(°) | $\Phi_1$/(°) | $d_2$/(Å) | $\theta_2$/(°) | $\Phi_2$/(°) |
| HF | 1.5763 | 113.2 | 167.9 | 1.5220 | 109.5 | 168.6 |
| $H_2O$ | 1.8445 | 111.1 | 159.4 | 1.7887 | 108.6 | 161.1 |
| *p*-fluorophenol | 1.7441 | 116.1 | 166.4 | 1.6870 | 112.1 | 167.4 |

[a] B3LYP/6-311++G(3df,3pd) level.

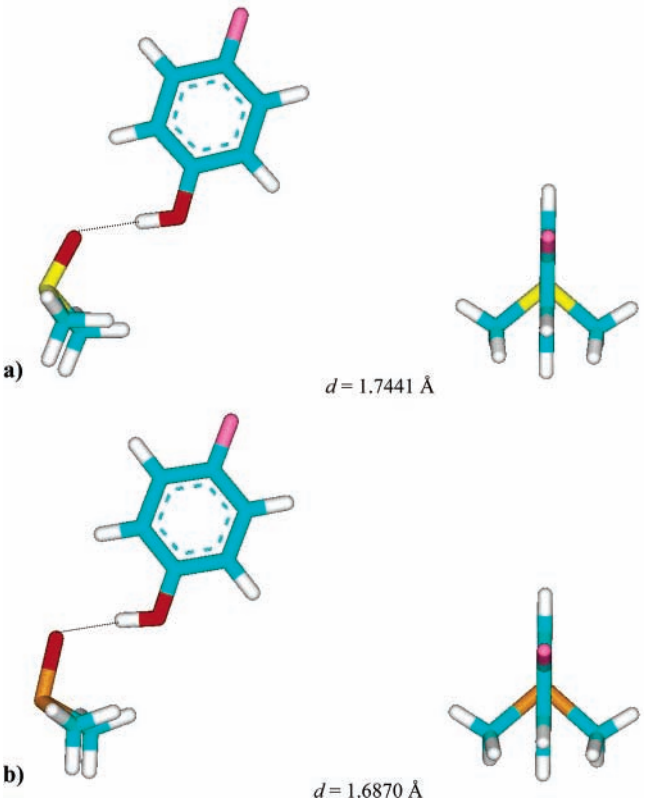


**Figure 6.** Optimized geometries (B3LYP/6-311++G(3df, 3pd) level) of the HB complexes of a) DMSO and b) DMSeO with *p*-fluorophenol.

*3.2.2. DMSO and DMSeO Hydrogen-Bonded Complexes.* 3.2.2.1. Geometries. Table 8 reports selected HB parameters of the DMS(Se)O complexes with HF, $H_2O$, and *p*-fluorophenol optimized at the B3LYP/6-311++G(3df,3pd) level. Figure 6 shows, as an example of the optimized geometries, one of the *p*-fluorophenol complexes (the same is obtained for the others HB donors). The HB parameters are the computed distances $d_1$ and $d_2$, the directionalities $\theta_1$ and $\theta_2$, and the linearities $\Phi_1$ and $\Phi_2$. These theoretical structural data show that, whatever the

**TABLE 9: NBO Descriptors[a] Computed[b] for the DMS(Se)O···HF Complexes**

| | q | | |
|---|---|---|---|
| | DMSO | DMSeO | $\Delta q^c$ |
| $n1_O$ | 1.9704 | 1.9758 | 0.0054 |
| $n2_O$ | 1.8737 | 1.8740 | 0.0003 |
| $n3_O$ | 1.8557 | 1.8895 | 0.0338 |
| $\sigma^*_{S(Se)-C1}$ | 0.0857 | 0.0780 | −0.0077 |
| $\sigma^*_{S(Se)-C2}$ | 0.0849 | 0.0775 | −0.0074 |
| $\sigma^*_{HF}$ | 0.0711 | 0.0881 | 0.0170 |
| | $E_{n\rightarrow\sigma^*}$ | | |
| | DMSO | DMSeO | $\Delta E_{n\rightarrow\sigma^*}$[d] |
| $n1_O \rightarrow \sigma^*_{HF}$ | 34.9 | 29.5 | −5.4 |
| $n2_O \rightarrow \sigma^*_{HF}$ | 111.5 | 163.0 | 51.4 |
| $n2_O \rightarrow \sigma^*_{S(Se)C}$[e] | 18.3 | 13.8 | −4.5 |
| $n3_O \rightarrow \sigma^*_{S(Se)C}$[e] | 43.2 | 33.3 | −9.9 |

[a] The values of the various descriptors are given in atomic units, and the energies are given in kJ/mol. [b] B3LYP/6-311++G(3df,3pd) level. [c] $\Delta q = q$NBO (DMSeO···HF) − $q$NBO (DMSO···HF). [d] $\Delta E_{n\rightarrow\sigma^*} = E_{n\rightarrow\sigma^*}$ (DMSeO···HF) − $E_{n\rightarrow\sigma^*}$ (DMSO···HF). For the n → $\sigma^*$ delocalizations associated with HB interactions, the difference is calculated by considering the sum of the two $n_O \rightarrow \sigma^*_{HF}$ transitions. [e] The values correspond to the mean of the $n_O \rightarrow \sigma^*_{S(Se)-C1}$ and $n_O \rightarrow \sigma^*_{S(Se)-C2}$ transitions (the atom numbering refers to that used in Figure 1).

HB donor, the HB are always shorter (stronger) for DMSeO, the corresponding shortening being consistently close to 0.0557 Å. Another interesting feature worth noting is the tendency, despite being insignificant, of the DMSeO HB to be more linear, a second characteristic typical of a stronger HB. Furthermore, this geometry corresponds to the global minimum found by Kirchner et al. in their investigation of 1DMSO−$n$H$_2$O Clusters.[3] Finally, it is worth noticing that the HB directionalities investigated through the $\theta$ HB angles are significantly smaller (in Table 8, $\theta$ varies from 109 to 116°) than the CSD angles (close to 130°). This lack of good quantitative agreement between theoretical and mean crystallographic HB angles has already been observed by Platts and co-workers in their investigation of the HB directionality to sulfur and oxygen compounds.[44] Such difference is to be expected given the diversity of complexes considered in the solid state, which often have bulky substituents compared to the methyl groups of DMS(Se)O considered in our DFT calculations.

3.2.2.2. NBO Descriptors. Table 9 shows the occupation numbers, calculated at the B3LYP/6-311++G(3df,3pd) level, for the DMS(Se)O···HF complexes of (i) the three lone pairs around the oxygen atoms, (ii) the $\sigma^*_{S(Se)-C}$ antibonding NBO paired with oxygen lone pairs through hyperconjugation, and (iii) the $\sigma^*_{HF}$ antibonding NBO paired with oxygen lone pairs through HB interactions. The stabilization energies corresponding to the various $n_O \rightarrow \sigma^*$ transitions and calculated through second-order perturbation theory are also indicated. The energies of the three oxygen lone pairs ($n1_O$, $n2_O$, and $n3_O$) of DMSO and DMSeO HB complexes and the corresponding percentage of p character (indicated in brackets) are, respectively, −0.81 (25,9%); −0.33 (96.1%); −0.30 (99.4%) and −0.80 (24,1%); −0.35 (91.1%); −0.29 (99.5%). The comparison of the NBO data calculated for 'free' (Table 7) and hydrogen-bonded (Table 9) DM(Se)O shows that in the HB complexes, the oxygen lone pair NBOs have an occupation number always inferior to the one in the 'free' molecules. As expected, the occupation of the antibonding $\sigma^*_{S(Se)-C}$ NBO follows the same trend. These results illustrate the competition between hyperconjugation and hydrogen-bonding in the $n_O \rightarrow \sigma^*$ transitions characteristic of the electronic structure of the HB complexes. The DMSO and DMSeO data compiled in Table 9 show that in the HB complexes the $n_O \rightarrow \sigma^*_{S(Se)-C}$ charge-transfer interactions follow the same behavior as in the free molecules. The examination of the data relative to the $n_O \rightarrow \sigma^*_{HF}$ interactions show that these delocalization effects are significantly more important in DMSeO since (i) the occupation number of the $\sigma^*_{HF}$ NBO is significantly greater in DMSeO and (ii) the stabilization energy, $E_{nO} \rightarrow \sigma^*_{HF}$ (calculated by considering the sum of the two $n_O \rightarrow \sigma^*_{HF}$ transitions), of the transitions associated with hydrogen bonding is about 46 kJ/mol greater in DMSeO than in DMSO. It is worth noticing from Table 9 that, among the NBO lone pairs involved in the $n_O \rightarrow \sigma^*_{HF}$ transitions ($n1_O$ and $n2_O$), the one having the highest p character ($n2_O$) leads to a much stronger $E_{nO} \rightarrow \sigma^*_{HF}$ energy (is therefore much more efficient) than the sp-type oxygen lone pair. This is coherent with the smaller NBO energy difference between the $\Delta\epsilon$ ($n_O$,$\sigma^*_{HF}$) for $n2_O$ (see eq 1).

**TABLE 10: HB Energetics (kJ/mol) of the Optimized[a] Complexes of DMS(Se)O with HF, H$_2$O, and *p*-Fluorophenol**

| | DMSO | | | DMSeO | | |
|---|---|---|---|---|---|---|
| HB donor | $-\Delta E_{el}$ | $-\Delta H^\circ_{298}$ | $-\Delta G^\circ_{298}$ | $-\Delta E_{el}$ | $-\Delta H^\circ_{298}$ | $-\Delta G^\circ_{298}$ |
| HF | 55.0 | 48.9 | 12.9 | 67.2 | 59.5 | 21.9 |
| H$_2$O | 32.7 | 25.7 | −9.8 | 39.3 | 32.3 | −4.6 |
| *p*-fluorophenol | 40.2 | 33.5 | −3.6 | 48.4 | 42.0 | 2.4 |

[a] B3LYP/6-311++G(3df,3pd)//B3LYP/6-311++G(3df,3pd) level.

3.2.2.3. Thermodynamic Quantities. To investigate the influence of the basis set enlargement on the energetics of the HB interactions in DMS(Se)O, we have used different levels of theory. The importance of the number of polarization and diffuse functions, already noticed on properties of the 'free' molecules, has been confirmed in the complexes since the BSSE calculated for the DMS(Se)O···HF systems at the B3LYP/6-311+G**//B3LYP/6-311+G** and at the B3LYP/6-311++G(3df,3pd)//B3LYP/6-311++G(3df,3pd) levels are, respectively, about −4.4 (−1.5) kJ/mol and −3.3 (−1.3) kJ/mol. Table 10 compiles the energetic parameters (variation of (i) electronic energy, $\Delta E_{el}$, (ii) enthalpy, $\Delta H^\circ_{298}$, and (iii) free energy, $\Delta G^\circ_{298}$, calculated at the B3LYP/6-311++G(3df,3pd)//B3LYP/6-311++G(3df,3pd) level. A first examination of the data of Table 10 shows that the evolution of the HB energetics for DMS(Se)O follows the acidity of the HB donor: HF > *p*-fluorophenol > H$_2$O. Whatever the HB donor and the energetic descriptor, DMSeO appears always as the better HB acceptor. The preference for DMSeO is ranging from about 10.6 to 6.6 kJ/mol for HF and H$_2$O, respectively, according to the $\delta\Delta H^\circ_{298}$ and from 9 to 5.2 kJ/mol toward the same HB donors according to the $\delta\Delta G^\circ_{298}$. If the same parameters are calculated for the complexes with *p*-fluorophenol, the respective values of $\delta\Delta H^\circ_{298}$ and $\delta\Delta G^\circ_{298}$ are 8.5 and 6.0 kJ/mol. They are in reasonable agreement with the experimental data available with *p*-fluorophenol since the corresponding values obtained through thermodynamic measurements in $CCl_4$ solutions are, respectively, 2.8 and 5.0 kJ/mol.[9] The overestimation of the computed $\delta\Delta H^\circ_{298}$ can be partly attributed to the neglect of solvent effects.

3.2.2.4. IR Frequency Shifts. The lowering of the $\nu$(XH) frequency of the HB donor on going from the free to the hydrogen-bonded XH group is probably one of the most used and sensitive probes of the strength of hydrogen-bonding interactions. We have, therefore, calculated the $\Delta\nu$(XH) frequency shifts corresponding to the various HB donors used in the complexation with DMSO and DMSeO. These data are

**TABLE 11: Theoretical Frequency Shifts $\Delta\nu$(XH) ($cm^{-1}$) Calculated[a] for the DMS(Se)O HB Complexes**

| HB donor | DMSO | DMSeO |
|---|---|---|
| HF | 882 | 1139 |
| $H_2O$ | 339[b] | 450[b] |
| *p*-fluorophenol | 449 | 608 |

[a] B3LYP/6-311++G(3df,3pd)//B3LYP/6-311++G(3df,3pd) level. [b] $\Delta\nu(\mathrm{OH}) = \Delta\nu(\text{free OH}) - \Delta\nu(\text{complex OH})$, with $\Delta\nu(\text{free OH}) = \sqrt{\frac{(\nu_s^2 + \nu_{as}^2)}{2}}$.

reported in Table 11. The computed spectroscopic quantities follow the energetic trends since (i) they are coherent with the order of HB donor acidity ($\Delta\nu$(HF) > $\Delta\nu$(OH) (*p*-fluorophenol) > $\Delta\nu$(OH) ($H_2O$)) and (ii) whatever the HB donor, the frequency shifts are always significantly greater for DMSeO. The $\delta\Delta\nu$(XH) have respective values of 257, 159, and 111 $cm^{-1}$ for HF, *p*-fluorophenol, and methanol. The value of 111 $cm^{-1}$ calculated for water compares well with the $\delta\Delta\nu$(OH) of about 110(±20) $cm^{-1}$ observed experimentally in $CCl_4$.[45]

## Conclusion

For the first time, we have characterized, through various complementary approaches, the relative hydrogen-bonding properties of sulfoxides and selenoxides. We have consistently found that selenoxides are better HB acceptors than sulfoxides. To the four questions addressed in the Introduction, we can now give the following answers:

(1) The significantly shorter HB measured in the solid state through the database investigation for SeO···HX interactions (1.78 (3) Å) in comparison with SO···HX HB (1.85 (2) Å) shows that selenoxides are better HB acceptors than sulfoxides.

(2) The database study reveals that the directionalities and linearities of HBs in sulfoxides and selenoxides are very similar. The stereochemistry of hydrogen bonding on sulfoxides is trans-trans (relative to the X−S bonds), a trend coherent with the directional preferences observed for metal(M)−oxygen coordination in these systems.

(3) The analysis of the molecular electrostatic potentials of DMSO and DMSeO calculated through density functional density indicates that the better HB ability of selenoxides can partly be attributed to the increased electron density on the oxygen of DMSeO compared to DMSO. The electronic structure of the two models investigated through an NBO analysis allows light to be shed on this behavior since negative hyperconjugation of the type $n_O \rightarrow \sigma^*_{S(Se)-C}$ appears to be significantly less important in DMSeO.

(4) Despite the known importance of environmental effects, the various experimental data available (i) in the solid state, geometries of HB complexes for SO···HX and SeO···HX molecular fragments and (ii) in $CCl_4$ solution, $\delta\Delta G^\circ_{298}$, $\delta\Delta H^\circ_{298}$ and $\Delta\nu$(OH) frequency shifts, are in reasonable agreement with the gas-phase computational data obtained at the B3LYP/6-311++G(3df, 3pd)//B3LYP/6-311++G(3df, 3pd)) level through the study of various DMS(Se)O···HX HB complexes.

**Acknowledgment.** The authors wish to thank Dr. Tore Brinck for access to the HS95 package. The authors also gratefully acknowledge the IDRIS (Institut du Développement et des Ressources en Informatique Scientifique), the CINES (Centre Informatique National de l'Enseignement Supérieur), and the CCIPL (Centre de Calcul Intensif des Pays de la Loire) for a grant of computer time.

## References and Notes

(1) For example: (a) Martin, D.; Weise, A.; Niclas H.-J. *Angew. Chem., Int. Ed. Engl.* **1967**, *6*, 318. (b) Luzar, A.; Soper, A. K.; Chandler, D. *J. Chem. Phys.* **1993**, *99*, 6836. (c) Soper, A. K.; Luzar, A. *J. Phys. Chem.* **1996**, *100*, 1357. (d) Borin, I. A.; Skaf, M. S. *Chem. Phys. Lett.* **1998**, *296*, 125. (e) Kirchner, B.; Searles, D. J.; Dyson, A. J.; Vogt, P. S.; Huber, H. *J. Am. Chem. Soc.* **2000**, *122*, 5379.

(2) For example: (a) Drago, R. S.; Wayland, B.; Carlson, R. L. *J. Am. Chem. Soc.* **1963**, *85*, 3125. (b) Ghersetti, S.; Lusa, A. *Spectrochim. Acta* **1965**, *21*, 1067. (c) Møllendhal, H.; Grundnes, J.; Klaboe, P. *Spectrochim. Acta* **1968**, *24A*, 1067. (d) Rostueso, P. *Finn. Chem. Lett.* **1979**, 202. (e) Prezhdo, V. V.; Prezhdo, O. V.; Vaschenko, E. V. *J. Mol. Struct.* **1995**, *356*, 7.

(3) Kirchner, B.; Reiher, M. *J. Am. Chem. Soc.* **2002**, *124*, 6206.

(4) Wang, B.; Hinton, J. F.; Pulay, P. *J. Phys. Chem. A* **2003**, *107*, 4683.

(5) Vergenz, R. A.; Yazji, I.; Whittington, C.; Daw, J.; Tran, K. T. *J. Am. Chem. Soc.* **2003**, *125*, 12318.

(6) Calligaris, M.; Carugo, O. *Coord. Chem. Rev.* **1996**, *153*, 83.

(7) Geremia, S.; Calligaris, M.; Kukushkin, Y. N.; Zinchenko, A. V.; Kukushkin, V. Y. *J. Mol. Struct.* **2000**, *516*, 49.

(8) Renault, E.; Berthelot, M.; Laurence, C.; Le Questel, J.-Y. *J. Phys. Org. Chem.* submitted for publication.

(9) Steiner, T. *Angew. Chem., Int. Ed.* **2002**, *41*, 48.

(10) Dobado, J. A.; Martínez-García, H.; Molina, J.; Sundberg, M. R. *J. Am. Chem. Soc.* **1999**, *121*, 3156.

(11) Allen, F. H. *Acta Crystallogr.* **2002**, *B58*, 380.

(12) Bruno, I. J.; Cole, J. C.; Edgington, P. R.; Kessler, M.; Macrae, C. F.; McCabe, P.; Pearson, J.; Taylor, R. *Acta Crystallogr.* **2002**, *B58*, 389.

(13) *Quest User Guide*; Cambridge Crystallographic Data Centre: Cambridge, UK, 1994; 1995 for *Vista*.

(14) Allen, F. H.; Kennard, O.; Taylor, R.; Watson, D. G.; Orpen, A. G.; Brammer, L. L. *J. Chem. Soc., Perkin Trans. 2*, **1987**, S1.

(15) Desiraju, G. R.; Steiner, T. In *The Weak Hydrogen Bond In Structural Chemistry and Biology*; Oxford University Press: New York, 1999.

(16) Rowland, R. S.; Taylor, R. *J. Phys. Chem.* **1996**, *100*, 7384.

(17) Bondi, A. *J. Phys. Chem.* **1964**, *68*, 441.

(18) Cambridge Crystallographic Data Centre: Cambridge, UK, 1997.

(19) Rablen, P. R.; Lockman, J. W.; Jorgensen, W. L. *J. Phys. Chem. A* **1998**, *102*, 3782.

(20) Becke, A. D. *J. Chem. Phys.* **1996**, *104*, 1040.

(21) Sirois, S.; Proynov, E. I.; Nguyen, D. T.; Salahub, D. R. *J. Chem. Phys.* **1997**, *107*, 6770.

(22) Frisch, M. J.; Trucks, G. W.; Schlegel, H. B.; Scuseria, G. E.; Robb, M. A.; Cheeseman, J. R.; Zakrzewski, V. G.; Montgomery, J. A., Jr.; Stratmann, R. E.; Burant, J. C.; Dapprich, S.; Millam, J. M.; Daniels, A. D.; Kudin, K. N.; Strain, M. C.; Farkas, O.; Tomasi, J.; Barone, V.; Cossi, M.; Cammi, R.; Menucci, B.; Pomelli, C.; Adamo, C.; Clifford, S.; Ochterski, J.; Petersson, G. A.; Ayala, P. Y.; Cui, Q.; Morokuma, K.; Malick, D. K.; Rabuck, A. D.; Raghavachari, K.; Foresman, J. B.; Cioslowski, J.; Ortiz, J. V.; Baboul, A. G.; Liu, G.; Liashenko, A.; Piskorz, P.; Komaromi, I.; Gomperts, R.; Martin, R. L.; Fox, D. J.; Keith, T.; Al-Laham, M. A.; Peng, C. Y.; Nanayakkara, A.; Challacombe, M.; Gill, P. M. W.; Johnson, B.; Chen, W.; Wong, M. W.; Andres, J. L.; Gonzalez, C.; Head-Gordon, M.; Replogle, E. S.; Pople, J. A. *Gaussian 98*, revision A.9; Gaussian, Inc.: Pittsburgh, PA, 1998.

(23) For example, see: (a) Hussein, W.; Walker, C. G.; Peralta-Inga, Z.; Murray, J. S. *Int. J. Quantum Chem.* **2001**, *82*, 160. (b) Galabov, B.; Bobadova-Parvanova, P. *J. Phys. Chem. A* **1999**, *103*, 6793. (c) Brinck, T. *J. Phys. Chem. A* **1997**, *101*, 3408.

(24) For example, see: (a) Hagelin, H.; Murray, J. S.; Brinck, T.; Berthelot, M.; Politzer, P. *Can. J. Chem.* **1995**, *73*, 483. (b) Le Questel, J.-Y.; Berthelot, M.; Laurence, C. *J. Phys. Org. Chem.* **2000**, *13*, 347. (c) Graton, J.; Berthelot, M.; Laurence, C. *J. Chem. Soc., Perkin Trans 2*, **2001**, 2130. (d) Graton, J.; Berthelot, M.; Besseau, F.; Raczyńska, E. D.; Laurence, C. *Can. J. Chem.* **2002**, *80*, 1375.

(25) Bader, R. F. W.; Carroll, M. T.; Cheeseman, S. R.; Chang, C. *J. Am. Chem. Soc.* **1987**, *109*, 7968.

(26) Brinck, T.; Murray, J. S.; Politzer, P. *Int. J. Quantum Chem.* **1992**, *19*, 57.

(27) (a) Brinck, T. In *Theoretical Organic Chemistry*, Párkányi. C., Ed.; Theoretical and Computational Chemistry; Elsevier Science: Amsterdam, 1998; Vol. 5, p 51. (b) Haeberlein, M.; Brinck, T. *J. Chem. Soc., Perkin Trans. 2*, **1997**, 289. (c) Brinck, T.; Murray, J. S.; Politzer, P. *J. Org. Chem.* **1993**, *58*, 7070.

(28) Reed, A. E.; Curtiss, L. A.; Weinhold, F. *Chem. Rev.* **1988**, *88*, 899.

(29) Reed, A. E.; Schleyer, P. v. R. *J. Am. Chem. Soc.* **1990**, *112*, 1434.

(30) Leusser, D.; Hehn, J.; Kocher, N.; Engels, B.; Stalke, D. *J. Am. Chem. Soc.* **2004**, *126*, 1781.

(31) Alabugin, I. V.; Zeidan, T. A. *J. Am. Chem. Soc.* **2002**, *124*, 3475.
(32) Lamarche, O.; Platts, J. A. *Chem. Eur. J.* **2002**, *8*, 457.
(33) Laurence, C.; Berthelot, M. *Perspect. Drug Discovery Des.* **2000**, *18*, 39.
(34) For example, see: (a) Trindle, C.; Crum, P.; Douglass, K. *J. Phys. Chem. A* **2003**, *107*, 6236. (b) Kovács, A.; Szabó, A.; Nemcsok, D.; Hargittai, I. *J. Phys. Chem. A* **2002**, *106*, 5671. (c) Vorobyov, I.; Yappert, M. C.; DuPré, D. B. *J. Phys. Chem. A* **2002**, *106*, 668. (d) Kryachko, E. S.; Zeegers-Huyskens, T. *J. Phys. Chem. A* **2002**, *106*, 6832.
(35) Boys, S. F.; Bernardi, F. *Mol. Phys.* **1970**, *19*, 553.
(36) Van Duijneveldt, F. B.; van Duijneveldt-van de Rijdt, J. G. C. M.; van Lenthe, J. H. *Chem. Rev.* **1994**, *94*, 1873.
(37) Xantheas, S. S. *J. Chem. Phys.* **1997**, *107*, 6770.
(38) Feder, W.; Dreizler, H.; Rudolph, H. D.; Typke, V. *Z. Naturforsh. Teil A* **1969**, *24*, 266.
(39) Typke, V.; Dakkouri, M. *J. Mol. Struct.* **2001**, *599*, 177.
(40) Dikarev, E. V.; Petrukhina, M. A.; Li X.; Block, E. *Inorg. Chem.* **2003**, *42*, 1966.
(41) Fujiwara, T.; Tanaka, N.; Ooshita, R.; Hino, R.; Mori, K.; Toda, F. *Bull. Chem. Soc. Jpn.* **1990**, *63*, 249.
(42) Toda, F.; Tanaka, K.; Mak, T. C. W. *Chem. Lett.* **1984**, 2085.
(43) Procter, D. J.; Thornton-Pett, M.; Rayner, C. M. *Tetrahedron* **1996**, *52*, 1841.
(44) Platts, J. A.; Howard, S. T.; Bracke, B. R. F. *J. Am. Chem. Soc.* **1996**, *118*, 2726
(45) Luçon, M., private communication.